Available online at www.sciencedirect.com
SCIENCE DIRECT®
Microporous and Mesoporous Materials 80 (2005) 195–203
MICROPOROUS AND MESOPOROUS MATERIALS
www.elsevier.com/locate/micromeso

Benzylation of benzene and other aromatics by benzyl chloride over mesoporous AlSBA-15 catalysts

A. Vinu [a,*], Dhanashri P. Sawant [b], K. Ariga [c], M. Hartmann [d], S.B. Halligudi [b]

[a] International Center for Young Scientists, National Institute for Materials Science, 1-1 Namiki, Tsukuba, Ibaraki 305-0044, Japan
[b] National Chemical Laboratory, Pune, India
[c] Supermolecules group, Advanced Materials Laboratory, National Institute for Materials Science, 1-1 Namiki, Tsukuba, Ibaraki 305-0044, Japan
[d] Kaiserslautern University of Technology, D-67663, Kaiserslautern, Germany

Received 10 August 2004; received in revised form 6 December 2004; accepted 8 December 2004
Available online 22 January 2005

Abstract

Aluminum-containing mesoporous molecular sieves AlSBA-15 with different n_{Si}/n_{Al} ratios and AlMCM-41 have been synthesized hydrothermally and characterized in detail by physicochemical methods, viz. XRD, N_2 adsorption and ^{27}Al NMR spectroscopy. The low angle XRD and N_2 adsorption measurements reveal that the structural order of SBA-15 was retained after the incorporation of Al. The increase of the unit cell parameter with increasing aluminum content and ^{27}Al MAS NMR spectroscopy confirm the incorporation of aluminum in the framework. Benzylation of benzene and substituted benzenes reaction employing benzyl chloride as the alkylating agent over AlSBA-15 and AlMCM-41 have been investigated. The influence of various reaction parameters such as reaction temperature, reactant feed ratio and catalyst amount affecting the activity and selectivity of AlSBA-15, have been studied. Among the mesoporous catalysts studied, AlSBA-15(45), where the number in parentheses indicates the molar n_{Si}/n_{Al} ratio, shows both high conversion and high selectivity for the benzylation of benzene. The activity of this catalyst for the benzylation of different aromatic compounds is in the following order: benzene > toluene > *p*-xylene > mesitylene > anisole. Kinetics of the benzene benzylation over different catalysts have also been investigated.

Keywords: Benzylation; AlSBA-15; SBA-15; Alkylation

1. Introduction

The liquid phase benzylation of benzene and other aromatic compounds by benzyl chloride, hereafter indicated as BC, or benzyl alcohol is important for the production of diphenylmethane, denoted by DPM, and substituted diphenylmethanes which are industrially important compounds used as pharmaceutical intermediates and fine chemicals [1–4]. Such reactions are carried out industrially, using conventional strong homogeneous acid catalysts, such as $AlCl_3$, $FeCl_3$, BF_3, $ZnCl_2$ and H_2SO_4 [1,5]. However, these catalysts pose several problems, such as toxicity, potential danger in handling, difficulty in separation and recovery of the catalyst, the products isolation, disposal problems due to large amounts of acidic effluents, corrosion and their requirement in stoichiometric amounts. Thus, there has been lots of interest to replace these homogeneous catalysts by heterogeneous solid acid catalysts, which can be easily separable from the reactant mixture and reusable, and also having high activity for Friedel-Crafts type reactions. Earlier studies indicated that highly acidic zeolite catalysts, such as HY and H-ZSM-5, show poor activity for the benzylation reaction, because of diffusion

* Corresponding author. Tel.: +81 29 851 3354x8679; fax: +81 29 860 4706.
E-mail address: vinu.ajayan@nims.go.jp (A. Vinu).

1387-1811/$ - see front matter © 2005 Elsevier Inc. All rights reserved.
doi:10.1016/j.micromeso.2004.12.012

limitation caused by their microporous network [6,7]. Solid superacids based on sulfated zirconia also show poor activity in the benzylation of benzene and other aromatic compounds [8].

The discovery of the new family of mesoporous silica molecular sieves with pore diameters in the 2.0–10.0 nm range, designated as M41S, is of considerable interest for heterogeneous catalysis and material science [9]. This family of materials is characterized by a regular array of pores with uniform diameter, high specific surface areas and pore volumes, which are advantageous for the adsorption and catalysis. However, the materials consisting of pure-silica frameworks are of limited use for various catalytic applications because of the lack of acid sites and ion exchange capacity. The incorporation of aluminum within the silica framework of mesoporous materials has been implemented in order to increase their acidity, ion-exchange capacity, and catalytic activity. There are many reports of the synthesis and characterization of metal substituted mesoporous materials with different n_{Si}/n_{Al} ratios, with different alumina or silica sources [10–24]. The acidity has been determined by FT-IR spectroscopy after adsorption of ammonia or pyridine [13–21]. Weglarski et al. have observed an increase of Brønsted acidity up to a molar Si/Al ratio of 34 [13]. Mokaya et al. prepared materials with Si/Al = 6.8 and reported about a constant Brønsted to Lewis site ratio up to a molar Si/Al ratio of 10 [14–18]. Depending on the nature and number of aluminum atoms in the framework, both the density and strength of acid sites may be varied.

Choudhary et al. reported that $AlCl_3$ supported on Si-MCM-41 showed poor catalytic activity for the benzylation of benzene, whereas supported $FeCl_3$, $GaCl_3$ and $InCl_3$ were highly active [25–27]. On the contrary, Hu et al. found that $AlCl_3$/MCM-41 showed higher activity as compared to other metal chloride supported mesoporous catalysts, such as $ZnCl_2$/MCM-41, $FeCl_3$/MCM-41, $CuCl_2$/MCM-41 and $NiCl_2$/MCM-41 [28]. However, the metal chloride immobilized in the mesopores will block the pores partially or completely and thereby reduce the specific surface area, pore volume and pore diameter or play a negative role, such as leaching, catalytic poisoning or blocking the active sites in catalysis.

Highly ordered large pore mesoporous silica molecular sieves SBA-15 with considerably thicker pore walls as compared to MCM-41, have been recently synthesized using an amphiphilic tri-block copolymer as the structure directing agent in highly acidic media [29–32]. SBA-15 exhibits improved hydrothermal stability as compared to MCM-41 [9,30]. Yue et al. reported the direct synthesis of AlSBA-15 and found that catalytic activity of AlSBA-15 in cumene cracking is higher as compared to AlMCM-41 [33]. Very recently, Vinu et al. have successfully reported the synthesis of AlSBA-15 materials with high aluminum content and tunable pore diameters by simply adjusting the molar water to hydrochloric acid ratio (n_{H_2O}/n_{HCl}) [34,35]. In this work, we report the benzylation of benzene and substituted benzene by benzyl chloride over large pore mesoporous AlSBA-15 catalysts with different aluminum contents and AlMCM-41. AlSBA-15 materials with different n_{Si}/n_{Al} ratios were successfully synthesized by a hydrothermal process using tri-block copolymer as template in a highly acidic medium and characterized by XRD, AAS, N_2 adsorption, TGA-TPD and its catalytic activity was tested in the benzylation of benzene.

2. Experimental section

2.1. Materials

Aluminum isopropoxide and tetraethyl orthosilicate (TEOS) (Merck) were used as the source for aluminum and silicon respectively. Tri-block copolymer poly(ethylene glycol)-*block*-poly(propylene glycol)-*block*-poly(ethylene glycol) (Pluronic P123, molecular weight = 5800, $EO_{20}PO_{70}EO_{20}$) (Aldrich) was used as structure directing template. *m*-Cresol and isopropanol were purchased from Merck and used without further purification.

2.2. Preparation of the catalysts

AlSBA-15 samples with different n_{Si}/n_{Al} ratios were syn- thesized using tri-block copolymer, poly(ethylene glycol)-*block*-poly(propylene glycol)-*block*-poly(ethylene glycol) as a structure directing agent with the following molar gel composition: TEOS:0.02–0.15Al_2O_3:0.016P123:0.46HCl:127H_2O. In a typical synthesis, 4 g of Pluronic P123 was added to 30 ml of water. After stirring for a few hours, a clear solution was obtained. 70 g of 0.28 M hydrochloric acid was added to it and the solution was stirred for another 2 h. Then, 9 g of tetraethyl orthosilicate and the required amount of aluminum source were added and the resulting mixture was stirred for 24 h at 40 °C. The solid product was recovered by filtration, washed with water for several times, and dried overnight at 100 °C. Finally, the product was calcined at 540 °C to remove the template.

AlMCM-41(23), where the number in the parentheses indicates the n_{Si}/n_{Al} molar ratio was synthesized from gels with the following gel composition: 10SiO_2:5.4C_nTMABr:0.2173Al_2O_3:3.2716Na_2O:1.3H_2SO_4:480H_2O. A typical synthesis procedure for AlMCM-41(23) using tetradecyltrimethylammonium bromide is as follows: 32 g of tetradecyltrimethylammonium bromide and 115 g of water was mixed and stirred for 30 min. Thereafter, 37.4 g of sodium silicate solution was added drop wise to the surfactant solution under vigorous stirring. After stirring for another 30 min, 0.7 g of sodium aluminate was dissolved in 5 ml of water, added to the synthesis mixture and the resulting gel was stirred for another

15 min. Then 2.4 g of conc. H_2SO_4 in 10 g of water was added to the above mixture to reduce the pH to ca. 11.5. The stirring was continued for another 30 min and the resulting gel was transferred into a polypropylene bottle and kept in an oven at 100 °C for 24 h. After cooling to room temperature, the resultant solid was recovered by filtration, washed with distilled water and dried in an oven at 100 °C for 6 h. Finally, the materials were calcined in a muffle furnace at 540 °C for 10 h.

2.3. Characterization

The powder X-ray diffraction patterns of AlSBA-15 and AlMCM-41 materials were collected on a Siemens D5005 diffractometer using CuKα ($\lambda = 0.154$ nm) radiation. The diffractograms were recorded in the 2θ range of 0.8–10° with a 2θ step size of 0.01° and a step time of 10 s. Nitrogen adsorption and desorption isotherms were measured at −196 °C on a Quantachrome Autosorb 1 sorption analyzer. The samples were outgassed for 3 h at 250 °C under vacuum in the degas port of the adsorption analyzer. The specific surface area was calculated using the BET model. Solid state ^{27}Al MAS NMR experiments were performed at room temperature on a Bruker MSL 500 NMR spectrometer with a resonance frequency of 130.32 MHz, applying a short 2.1 μs pulse and a recycle delay of 100 ms. Typical rotation frequency was about 10 kHz using a 4 mm diameter zirconia rotor. 12,500 scans were necessary to obtain a well resolved spectrum.

The density and strength of acid sites of AlSBA-15 and AlMCM-41(23) materials were determined by temperature-programmed-desorption (TPD) of pyridine. About 100 mg of the materials was evacuated for 3 h at 250 °C under vacuum ($p < 10^{-5}$ h Pa). Thereafter, the samples were cooled to room temperature under dry nitrogen followed by exposure to a stream of pyridine in nitrogen for 30 min. Subsequently, the physisorbed pyridine was removed by heating the sample to 120 °C for 2 h in a nitrogen flow. The temperature-programmed desorption (TPD) of pyridine was performed by heating the sample in a nitrogen flow (50 ml/min) from 120 to 700 °C at a rate of 10 °C/min using a high-resolution thermo-gravimetric analyzer (SETARAM setsys 16MS). The observed weight loss was used to quantify the number of acid sites assuming that each mole of pyridine corresponds to one mole of protons.

2.4. Catalytic studies

Anhydrous A.R. grade chemicals were used without further purification. The liquid phase benzylation of benzene with benzyl chloride (BC) was carried out in a 50 ml two necked flask attached to a condenser and a septum. The temperature of the reaction vessel was maintained using an oil bath. In a typical run, benzene and BC were added in the required molar ratio to the activated catalyst. The catalysts were activated at 500 °C in air for 4 h with a flow rate of 50 ml/min and cooled to room temperature prior to their use in the reaction. The reaction mixture was magnetically stirred and heated to the required temperature under atmospheric pressure. Samples were withdrawn at regular intervals of time and analyzed periodically on a gas chromatograph (HP-6890) equipped with a FID detector and a capillary column. The products were also identified by GC-MS (HP-5973) analysis. Since benzene was in excess, conversion was calculated based on the benzylating reagent i.e. BC.

3. Results and discussion

3.1. Characterization

The powder XRD patterns of calcined AlSBA-15(45), AlSBA-15(7) and AlMCM-41(23) samples are shown in Fig. 1. AlSBA-15(45) and AlSBA-15(7) show all the four well resolved peaks, which are indexed to (1 0 0), (1 1 0), (2 0 0) and (2 1 0) reflections of ordered hexagonal space group p6mm. The length of the hexagonal unit cell a_0 is calculated using the formula $a_0 = 2d_{100}/\sqrt{3}$. The observed d spacings are compatible with the hexagonal p6mm space group. It is interesting to note that the unit cell parameter increases significantly with the increase of aluminum content in the synthesis gel (Table 1), which could suggest the presence of aluminum in the SBA-15 walls. Elemental composition of AlSBA-15 materials is also presented in Table 1. In all cases, the n_{Si}/n_{Al} ratio of the calcined materials is higher than the n_{Si}/n_{Al} ratio in the synthesis gel. This could be due to the high solubility of the aluminum source in the acidic medium. The XRD powder pattern of AlMCM-41(23) also exhibits a

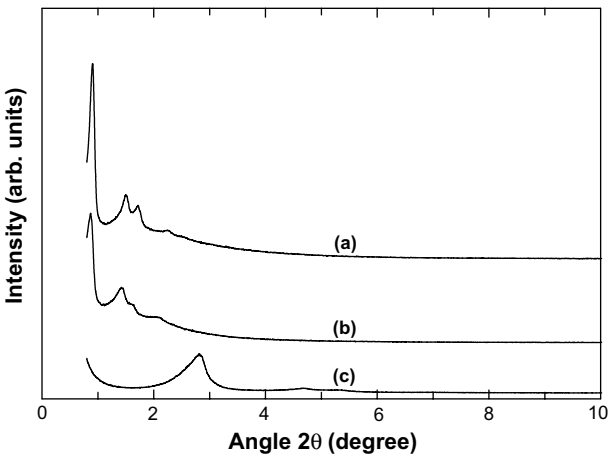

Fig. 1. XRD powder patterns of calcined AlSBA-15 with different n_{Si}/n_{Al} ratios and AlMCM-41(23): (a) AlSBA-15(45), (b) AlSBA-15(7) and (c) AlMCM-41(23).

Table 1
Textural parameters of AlSBA-15(45), AlSBA-15(7) and AlMCM-41(23) samples

Sample	a_0 (nm)	n_{Si}/n_{Al}		A_{BET} (m^2/g)	Pore volume (cm^3/g)	Pore diameter, $d_{p,ads}$ (nm)
		Gel	Product			
AlSBA-15(45)	11.27	7	45	930	1.35	9.7
AlSBA-15(7)	11.76	3	7	604	1.26	11.8
AlMCM-41(23)	3.63	23	22	1210	0.80	2.4

high degree of structural ordering as evident from the narrow (1 0 0) reflection and the presence of the higher order (1 1 0) and (2 0 0) reflections which can be indexed on a hexagonal lattice in good agreement with reported patterns of MCM-41 materials.

The nitrogen adsorption–desorption isotherms of AlSBA-15(45), AlSBA-15(7) and AlMCM-41(23) samples are shown in Fig. 2. AlSBA-15(45) and AlSBA-15(7) exhibit isotherms of type IV of the IUPAC classification featuring a narrow step due to capillary condensation of N_2 in the primary mesopores. In the case of AlSBA-15 materials, a steep increase and a H1-type hysteresis loop occur in the curve at a relative pressure of $0.65 < p/p_0 < 0.9$ due to the capillary condensation and desorption of nitrogen, which strongly suggest the presence of large mesopores in the AlSBA-15 samples. The amount of aluminum in the AlSBA-15 materials has a consequential impact on the BET specific surface area, specific pore volume and pore size of the AlSBA-15 materials. AlSBA-15(45) and AlSBA-15(7) possess pores with diameters of about 9.7 and 11.8 nm, high BET surface areas of 930 and 604 m^2/g, and large pore volumes of 1.35 and 1.26 cm^3/g, respectively. The decrease of specific pore surface area and pore volume with increasing aluminum content might suggest the presence of aluminum oxide species inside the mesopores of AlSBA-15. AlMCM-41(23) also exhibits a type IV isotherm which is typical for MCM-41, with a capillary condensation step at a relative pressure of $0.22 < p/p_0 < 0.32$. The absence of hysteresis loop in the desorption branch suggests that no interparticle mesoporosity is present. The BET specific surface area, pore volume and the BJH pore diameter for AlMCM-41(23) are 1210 cm^2/g, 0.80 cm^3/g and 2.4 nm, respectively (Table 1).

The ^{27}Al MAS NMR spectra of the calcined AlSBA-15(45), AlSBA-15(7) and AlMCM-41(23) samples are shown in Fig. 3. It can be seen that the coordination of Al atom was significantly affected with the increasing n_{Si}/n_{Al} ratio in the product. All samples prepared up to the n_{Si}/n_{Al} ratio 45 show only tetrahedral coordination. However, the coordination of the Al atoms is changed below the n_{Si}/n_{Al} ratio of 45. AlSBA-15(7) shows a sharp peak centered around 53 ppm and two small peaks centered around 7 ppm and 22 ppm. The peak at 53 ppm is assigned to Al in tetrahedral environment (AlO_4 structural unit, Al(tet)), in which Al is covalently bound to four Si atoms via oxygen bridges. The peaks corresponding to 22 ppm and 7 ppm are attributed to penta- and hexa-coordinated aluminum which might have formed by leaching during calcination. AlMCM-41(23) also exhibits a signal with a chemical shift of ca. 52 ppm characteristics of aluminum in tetrahedral coordination and a small shoulder at 0 ppm, which suggests that a small amount of aluminum occupies octahedral coordination.

The density and strength of the acid sites were determined using temperature-programmed-desorption (TPD) of pyridine and the data are presented in Table 2. Weak (weight loss between 220 and 350 °C), moderate (350 °C–450 °C) and strong (450–600 °C) acid sites are found in all samples. The weak acid sites are attributed to surface hydroxyl groups, and the medium and strong acid sites

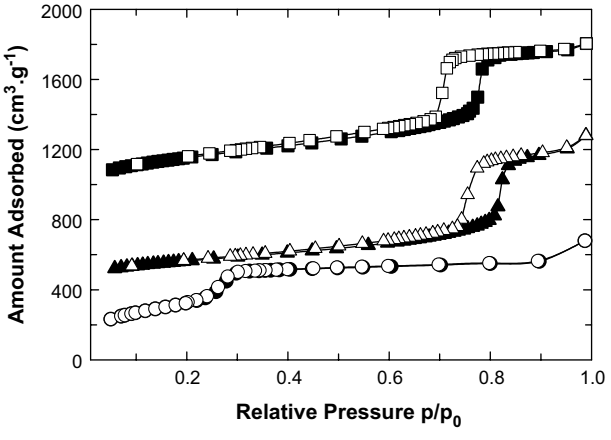

Fig. 2. Nitrogen adsorption isotherms (adsorption: closed symbols; desorption: open symbols) of AlSBA-15 with different n_{Si}/n_{Al} ratios and AlMCM-41 materials: (■) AlSBA-15(45), (▲) AlSBA-15(7) and (●) AlMCM-41(23). The isotherms are shifted by 400 cm^3/g upward for clarity.

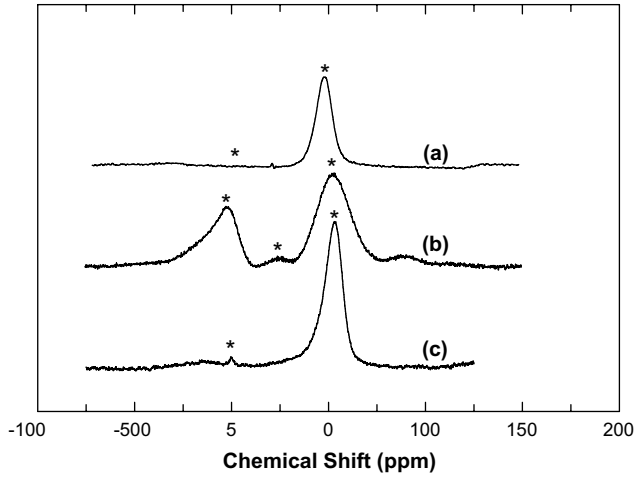

Fig. 3. ^{27}Al MAS NMR spectra of calcined AlSBA-15 with different n_{Si}/n_{Al} ratios: (a) AlSBA-15(45), (b) AlSBA-15(7) and (c) AlMCM-41(23).

Table 2
Density and strength of acid sites of AlSBA-15(45), AlSBA-15(7) and AlMCM-41(23) samples

Catalyst	Acid sites/mmol g^{-1}			
	Weak (220–350 °C)	Moderate (350–450 °C)	Strong (450–600 °C)	Total (>350 °C)
AlSBA-15(45)	0.418	0.182	0.257	0.439
AlSBA-15(7)	0.241	0.248	0.139	0.387
AlMCM-41(23)	0.754	0.088	0.271	0.359

originate from the incorporation of aluminum atoms into the SBA-15 walls. It is very interesting to note that, as n_{Si}/n_{Al} ratio increases, the number of weak acids sites which comes from the weakly held hydrogen-bonded pyridine on terminal silanol group increases. This is consistent with the fact that the concentration of terminal silanol groups per fixed weight of samples is expected to increase with the n_{Si}/n_{Al} ratio. However, the medium acid sites decrease with increase of n_{Si}/n_{Al} ratio. It should also be noted that the total number of acid sites (medium and strong acid sites) in AlSBA-15 also increases with increasing n_{Si}/n_{Al} ratio. Moreover, the acidity data of AlSBA-15 materials is compared with acidity data obtained from AlMCM-41(23) and the results are also given in Table 2. The total number of acid sites of the materials used in this study decreases in the following order: AlSBA-15(45) > AlSBA-15(7) > AlMCM-41(23).

3.2. Catalytic activity

The conversion of benzyl chloride (BC) in the benzylation of benzene over AlSBA-15 catalyst with different n_{Si}/n_{Al} ratios and AlMCM-41(23) is shown in Fig. 4a. The products obtained are diphenylmethane (DPM) and the isomers of dibenzylbenzene (DBB) such as 1,4-DBB, 1,3-DBB and 1,2-DBB. Fig. 4b shows that upon rising conversion of BC a decrease in the DPM occurs. For AlSBA-15, BC conversions of 75.5% and 98.8% and selectivities towards DPM of 78% and 81% were achieved after 9 h reaction at 80 °C over AlSBA-15(7) and AlSBA-15(45), respectively, indicating a very interesting catalytic activity of large pore mesoporous materials in the benzylation of benzene with BC. By contrast, AlMCM-41(23) registers only 23% BC conversion which is much lower than those obtained with the AlSBA-15 catalysts after 9 hours of reaction under the same reaction condition (Fig. 4b).

The rate data for the benzylation of benzene reaction in excess of benzene over AlSBA-15(45), AlSBA-15(7) and AlMCM-41(23) catalysts could be fitted well to a pseudo-first order rate law:

$$\log(1/1-x) = (k_a/2.303)(t-t_0)$$

where k_a is the apparent rate constant, x the fractional conversion of benzyl chloride, t the reaction time and t_0 the induction period corresponding to the time required for reaching equilibrium temperature. A plot of $\log[1/1-x]$ versus $(t-t_0)$ gives a linear plot over a range from 10% to 90%. The activity of the catalysts declines in the following order: AlSBA-15(45) > AlSBA-15(7) > AlMCM-41(23). The apparent rate constant for the benzylation reaction over AlSBA-15(45) amounts to $53.0\times10^{-4}\,min^{-1}$, that of AlSBA-15(7) is $34.6\times10^{-4}\,min^{-1}$, while AlMCM-41(23) registers an apparent rate constant of only $6.9\times10^{-4}\,min^{-1}$.

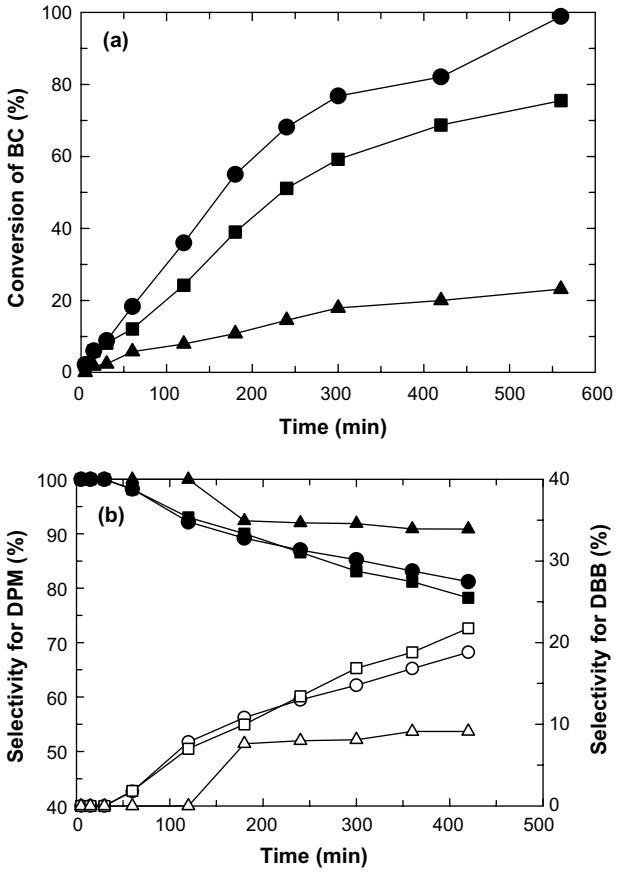

Fig. 4. (a) Benzyl chloride conversion in the benzylation of benzene over different catalysts at 80 °C, benzene to benzyl chloride ratio 10, reaction time 3 h: (●) AlSBA-15(45), (■) AlSBA-15(7) and (▲) AlMCM-41(23). (b) Product selectivities in the benzylation of benzene over different catalysts at 80 °C, benzene to benzyl chloride ratio 10, reaction time 3 h: (diphenylmethane selectivity: closed symbols; selectivity for the total isomers of dibenzylbenzene: open symbols): (●) AlSBA-15(45), (■) AlSBA-15(7) and (▲) AlMCM-41(23).

The main advantage of using large pore AlSBA-15 catalyst in this reaction is its higher thermal, hydrothermal and water stability as compared to other mesoporous catalysts [9,30]. The high benzylation activity of AlSBA-15(45) may be attributed to the presence of a small amount of non-framework Al oxide species (synthesized in a highly acidic medium) in combination with the strong acid sites. On the other hand, the low catalytic activity of AlSBA-15(7) as compared to that of AlSBA-15(45) can probably be attributed to a higher

important coverage of the SBA-15 pore wall surface by the aluminum species as evidenced by its low surface area and specific pore volume and a significant loss of the surface acid sites due to large amounts of extra-framework aluminum atoms. It is also assumed that some aluminum atoms are within the walls of SBA-15 and are not accessible to the reactant molecules. Moreover, it is interesting to note that on increasing the reaction time, the selectivity towards DPM over all the catalysts studied in this study is decreased with the concomitant increase of the selectivity for the isomers of DBB. With increasing the reaction time, a consecutive reaction between DPM and BC is occurred in the large pores of AlSBA-15. Thus, the increase in DBB selectivity is accompanied by a decrease in DPM selectivity. It is significant to note that the selectivity for 1,4-DBB is higher than that of 1,2-DBB and 1,3-DBB and increases with increasing reaction time (Fig. 1S). The increase in the selectivity for 1,4-DBB is probably due to the lower kinetic diameter of this para product as compared with other dibenzylated products.

Increasing the temperature has a strong effect on both conversion and the selectivity of DPM. The effect of temperature on the benzylation activity of AlSBA-15(45) is shown in Table 3 and the kinetic curves are shown in Fig. 5. The results show that the catalytic performance of the catalyst strongly increased with increasing the reaction temperature. It can be seen from Table 3 that at 70 °C the conversion of BC and the selectivity for DPM were 8.5% and 100%, respectively, and amount to 55% and 89% at 80 °C for a reaction time of 3 h. Upon increasing the reaction temperature up to 90 °C, the conversion was increased from 55% to 100% with decrease in the selectivity to DPM from 90% to 77%. The above results reveal that the conversion of BC and the selectivity towards DPM can be easily tuned by simply adjusting the reaction temperature. It is interesting to note that the apparent rate constant was increased from 11.5 to 175×10^{-4} min^{-1} with increasing the reaction temperature from 70 to 90 °C. The first order rate constants calculated from these curves give an Arrhenius plot (Fig. 6) leading to a value of the activation energy for the AlSBA-15(45) catalyst of 137.45 KJ mol^{-1}. It

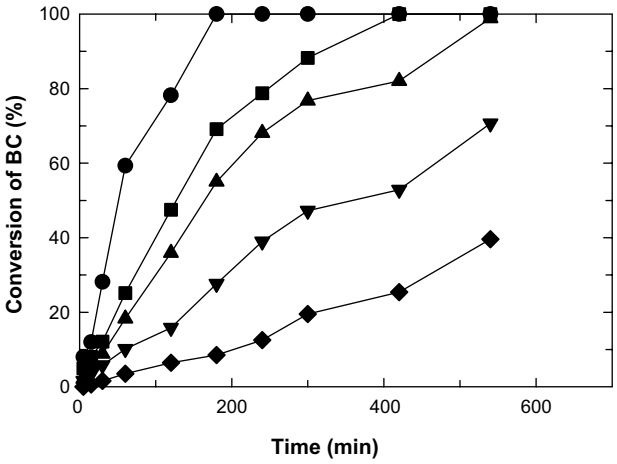

Fig. 5. Effect of reaction temperature on the conversion of benzyl chloride in the benzylation of benzene reaction over AlSBA-15(45) at (♦) 70 °C, (▼) 75 °C, (▲) 80 °C, (■) 85 °C and (●) 90 °C.

was previously reported that montmorillonite supported zinc (Clayzinc) with significant pore volumes and pores of diameter in the 10–12 nm range, which are generated by acid treatment, is highly active and can catalyze the above alkylation reaction even at room temperature [36,37]. Thus, the catalytic results of the AlSBA-15(45) catalyst imply that the activation energy for the above reaction over different catalysts with large pore diameters and pore volumes is not the same. Moreover, it is interesting to note that the selectivity to DBB increases with increasing the reaction temperature at the expense of the selectivity of DPM. This indicates that the consecutive alkylation reaction between the DPM and the BC molecules is enhanced at high reaction temperatures.

The influence of the stoichiometric ratio between benzene and BC for benzene benzylation reaction was studied over AlSBA-15(45) catalyst at a reaction temperature of 80 °C and a reaction time of 3 h. The product selectivity at various benzene to BC ratios is shown in Table 4. It is observed that conversion of BC increases by increasing benzene content. When the benzene to BC molar ratio increased from 5 to 15 the BC conversion is found to increase from 14.1% to 46.1%. It can also be seen from the Table 4 that the selectivity towards DPM is increased

Table 3
Catalytic activity of AlSBA-15(45) at different temperatures, reaction time of 3 h

Temperature (°C)	BC conversion (%)	Selectivity (%)					Apparent rate constant k_a ($\times 10^4$ min^{-1})
		DPM	Isomers of DBB				
			1,2-DBB	1,3-DBB	1,4-DBB	Total	
70	8.52	100	–	–	–	–	11.51
75	27.65	93.75	1.21	0.39	4.64	6.25	23.03
80	55.01	89.19	2.51	0.78	7.51	10.81	53.0
85	69.12	82.74	3.90	1.10	12.24	17.26	76.0
90	99.99	76.79	5.48	1.77	15.94	23.21	175.03

Amount of catalyst = 90 mg (3 wt% of total reaction mixture).

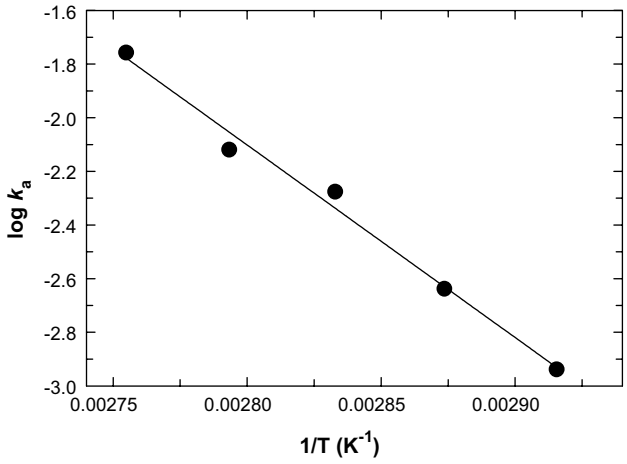

Fig. 6. Arrhenius plot of log$k$ a as a function of (1/T) for the benzylation of benzene over the AlSBA-15(45) catalyst.

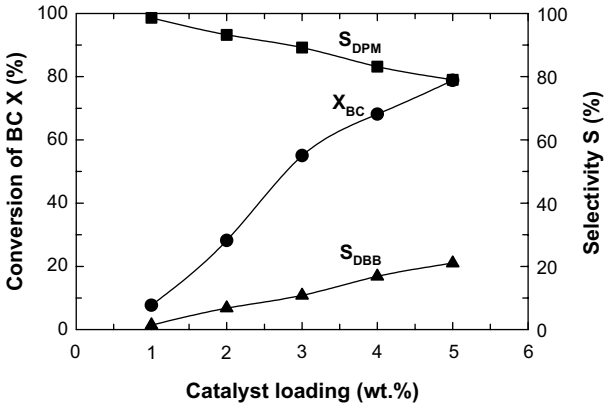

Fig. 7. Effect of catalyst loading on the conversion of benzyl chloride and product selectivities in the benzylation of benzene over AlSBA-15(45) at 80 °C, benzene to benzyl chloride ratio 10, reaction time 3 h: (●) X_{BC}, (■) S_{DPM} and (▲) S_{DBB}.

Table 4
Influence of the stoichiometric ratio between benzene and benzyl chloride for benzene benzylation over AlSBA-15(45) at a reaction temperature of 80 °C, reaction time of 3 h

Benzene to BC molar ratio	BC conversion (%)	Selectivity (%)			
		DPM	Isomers of DBB		
			1,2-DBB	1,3-DBB	1,4-DBB
5	14.10	86.23	3.02	1.02	9.73
7.5	29.98	87.88	2.89	0.99	8.24
10	55.01	89.19	2.51	0.78	7.52
15	46.12	100	–	–	–

Amount of catalyst = 90 mg (3 wt% of total reaction mixture).

with increasing benzene content. At benzene to BC ratio of 15, a selectivity of 100% can be achieved. The increase in BC conversion and DPM selectivity with increasing benzene to BC ratio can be attributed to the increased adsorption of benzene over the catalyst surface and higher dilution of BC. It is not surprising that the selectivity towards the DBB is decreased with decreasing the BC content.

The effect of catalyst loading on conversion and selectivity was studied between 1 and 5 wt.% of total reaction mixture over AlSBA-15(45) at a reaction temperature of 80 °C, time of 3 h and benzene to BC feed ratio of 10. It was observed that the selectivity of DPM was highly dependent on catalyst loading. With an increase in catalyst loading from 1 to 5 wt.%, the selectivity of DPM decreased from 98.6% to 79.0% respectively. BC conversion also increased from 7.7% to 78.9% when the catalyst loading increased from 1 to 5 wt.% (Fig. 7). It should also be noted that the formation of DBB was significantly increased with the increase of the catalyst concentration. This indicates the occurrence of the consecutive reactions between the DPM and the BC molecules over the active acidic sites of the AlSBA-15 catalyst.

The effect of electron donating substituent groups in the benzylation of benzene was also studied over AlSBA-15(45) at a reaction temperature of 80 °C, a substituted benzene to BC ratio of 10 and a reaction time of 3 h. The conversion and the yields of the isolated products of the benzylation of different aromatic compounds are given in Table 5. The BC conversion is decreased in the following order: benzene > toluene > *p*-xylene > mesitylene > anisole. The results indicate that the benzylation activity of the AlSBA-15(45) catalyst is decreased due to the presence of electron donating groups such as methyl and methoxy groups, in the aromatic substrate. The above observed result is totally opposite to the expected one, according to the classical mechanism of the Friedel-Crafts type acid catalyzed benzylation reaction, where the benzylation of an aromatic compound is easier if one or more electron donating groups are present in the aromatic ring [1]. Based on our reaction results, we assume that the AlSBA-15 catalyst shows a

Table 5
The effect of electron donating substituent groups in the benzylation of benzene over AlSBA-15(45) at a reaction temperature of 80 °C, substituted benzene to BC ratio of 10, reaction time of 3 h

Aromatic compound	BC conversion (%)	Major product selectivity (%)
Benzene	55.01	89.19[a]
Toluene	31.24	88.18[b]
p-Xylene	23.55	100[c]
Mesitylene	17.52	100[d]
Anisole	16.13	88.19[e]

Amount of catalyst = 90 mg (3 wt% of total reaction mixture).
[a] Diphenylmethane.
[b] 4-Methyl diphenylmethane.
[c] 2,5-Dimethyl diphenylmethane.
[d] 2,4,6-Trimethyl diphenylmethane.
[e] 4-Methoxy diphenylmethane.

possible poison effect by strong adsorption of the aromatic substrate. Obviously, the poison effect on the catalyst surface becomes larger when the electron density on the aromatic substrate is increased due to strong adsorption, resulting in a low activity. Similar effects have also been reported in the dealuminated HY zeolites on the acetylation of 2-methoxynaphthalene with acetic anhydride [38].

One of the advantages of using zeolite and mesoporous solid materials as catalysts is the possibility of their reusability and/or regeneration. When the reaction was carried out with pure siliceous SBA-15 catalyst and without any catalyst, no BC conversion was found. In order to study the heterogeneous nature of the reaction, a test reaction using AlSBA-15 catalyst was conducted. The reaction was stopped when the conversion reached 25% and the catalyst was removed by filtration. The filtrate was immediately reused in the benzylation of benzene and it was found that there was no increase in substrate conversion. In addition, the catalyst separated was reused after filtration with fresh reaction mixture and there was found no loss in its catalytic activity. These data are in agreement with the absence of catalyst leaching and a purely heterogeneous and not homogeneous catalysis. For testing catalytic activity of regenerated catalyst, used catalysts for the optimized reaction was removed by filtration, washed three times with A.R. grade acetone and then dried in an oven overnight at 100 °C. Then catalyst was activated at 500 °C for 4 h in an air flow and used for the above reaction. Same procedure was repeated twice or three times and the result of the reaction is given in Table 6. It was found from Table 6 that there is a very small change in the conversion of BC and selectivity towards DPM after two or three cycles. From the above results, it is concluded that the catalytic activity of AlSBA-15 can be maintained even after two or three cycles. It should also be noted that the structure of the AlSBA-15(45) was fully retained after multiple regeneration by calcination and could be attributed to its high wall thickness as compared to other mesoporous materials such as MCM-41 and MCM-48 [11,12].

Table 6
Effect of recycling of the catalysts in the benzylation of benzene with benzyl chloride at 80 °C

	BC conversion (%)	Selectivity (%)			
		DPM	Isomers of DBB		
			1,3-DBB	1,3-DBB	1,4-DBB
Fresh	55.01	89.19	2.51	0.78	7.52
I reuse	53.98	88.12	3.10	0.84	7.94
II reuse	51.99	89.55	2.25	0.75	7.45

Amount of catalyst = 90 mg (3 wt% of total reaction mixture), reaction time 3 h.

4. Conclusions

Aluminum-containing mesoporous molecular sieves AlSBA-15 with different n_{Si}/n_{Al} ratios were synthesized using aluminum isopropoxide as the source of aluminum and characterized by physicochemical methods, viz. XRD, N_2 adsorption and ^{27}Al NMR spectroscopy. The low angle XRD and N_2 adsorption measurements reveal that the structural order of SBA-15 was retained after the incorporation of Al in AlSBA-15 framework. The increase of the unit cell parameter with increasing aluminum content and ^{27}Al MAS NMR spectroscopy confirm the incorporation of aluminum in the framework. The catalytic activity of the AlSBA-15 catalyst with different n_{Si}/n_{Al} ratios was tested in the benzylation of benzene employing benzyl chloride as the alkylating agent and the results are compared with the AlMCM-41 catalyst. Among all catalyst studied, AlSBA-15(45) was the most active, showing high benzyl chloride conversion and selectivity to diphenylmethane. AlSBA-15(45) shows the following trend for its activity in the benzylation of benzene and substituted benzenes: benzene > toluene > *p*-xylene > mesitylene > anisole, which is totally opposite to that observed for the classical acid catalyzed Friedel-Crafts type benzylation reaction. The structure of the AlSBA-15 was fully retained after multiple regeneration by calcination. The activity and selectivity towards diphenylmethane hardly changed after three cycles.

Acknowledgments

A. Vinu is grateful to Prof. Y. Bando and Special Coordination Funds for Promoting Science and Technology from the Ministry of Education, Culture, Sports, Science and Technology of the Japanese Government for the award of ICYS Research Fellowship, Japan.

Supplementary data

Supplementary data associated with this article can be found, in the online version, at doi:10.1016/j.micromeso.2004.12.012.

References

[1] G.A. Olah, Friedel-Crafts Chemistry, Wiley, New York, 1973.
[2] R. Commandeur, N. Berger, P. Jay, J. Kervennal, EP 0442986, 1991.
[3] T.W. Bastock, J.H. Clark, Speciality Chemicals, Elsevier, London, 1991.
[4] B.M. Khadilkar, S.D. Borkar, Chem. Technol. Biotechnol. 71 (1998) 209.

[5] G.A. Olah, G.K.S. Prakash, J. Sommer, Superacids, Wiley-Interscience, New York, 1985.
[6] B. Coq, V. Gourves, F. Figueras, Appl. Catal. A 100 (1993) 69.
[7] V.R. Choudhary, S.K. Jana, B.P. Kiran, Catal. Lett. 59 (1999) 217.
[8] S.N. Koyande, R.G. Jaiswal, R.V. Jayaram, Ind. Eng. Chem. Res. 37 (1998) 908.
[9] C.T. Kresge, M.E. Leonowicz, W.J. Roth, J.C. Vartuli, J.S. Beck, Nature 359 (1992) 710.
[10] R. Schmidt, D. Akporiaye, M. Stöcker, O.H. Ellestad, J. Chem. Soc., Chem. Commun. (1994) 1493.
[11] Z. Luan, C.F. Cheng, H. He, J. Klinowski, J. Phys. Chem. 99 (1995) 10590.
[12] M. Busio, J. Jänchen, J.H.C. van Hooff, Micropor. Mater. 5 (1995) 211.
[13] J. Weglarski, J. Datka, H. He, J. Klinowski, J. Chem. Soc., Faraday Trans. 92 (1996) 5161.
[14] R. Mokaya, W. Jones, Z.H. Luan, M.D. Alba, J. Klinowski, Catal. Lett. 37 (1996) 112.
[15] R. Mokaya, W. Jones, J. Chem. Soc., Chem. Commun. (1996) 981.
[16] R. Mokaya, W. Jones, J. Chem. Soc., Chem. Commun. (1996) 983.
[17] R. Mokaya, W. Jones, J. Catal. 172 (1997) 211.
[18] R. Mokaya, W. Jones, J. Mater. Chem. 8 (1998) 2819.
[19] A. Vinu, K. Usha Nandhini, V. Murugesan, V. Umamaheswari, A. Pöppl, M. Hartmann, Appl. Catal. A-Gen. 265 (2004) 1.
[20] A. Vinu, K. Ariga, M. Saravanamurugan, M. Hartmann, V. Murugesan, Micropor. Mesopor. Mater. 76 (2004) 91.
[21] A. Vinu, T. Krithiga, V. Murugesan, M. Hartmann, Adv. Mater. 20 (2004) 1817.
[22] G. Øye, J. Sjöblom, M. Stöcker, Micropor. Mesopor. Mater. 27 (1999) 171.
[23] B. Bonelli, B. Onida, J.D. Chen, A. Galarneau, F. Di Renzo, F. Fajula, E. Garrone, Micropor. Mesopor. Mater. 67 (2004) 95.
[24] F. DiRenzo, B. Chiche, F. Fajula, S. Viale, E. Garrone, in: W. Hightower, W.N. Delgass, E. Eglesia, A.T. Bell (Eds.), 11th International Congress on Catalysis, 40th Anniversary, Stud. Surf. Sci. Catal., 101, Elsevier, Amsterdam, 1996, p. 851.
[25] V.R. Choudhary, S.K. Jana, B.P. Kiran, Catal. Lett. 64 (2000) 223.
[26] V.R. Choudhary, S.K. Jana, J. Mol. Catal. A: Chem. 180 (2002) 267.
[27] V.R. Choudhary, S.K. Jana, A.S. Mamman, Micropor. Mesopor. Mater. 56 (2002) 65.
[28] X. Hu, G.K. Chuah, S. Jaenicke, Appl. Catal. A-Gen. 217 (2001) 1.
[29] D. Zhao, Q. Huo, J. Feng, B.F. Chmelka, G.D. Stucky, J. Am. Chem. Soc. 120 (1998) 6024.
[30] P. Yang, D. Zhao, D. Margolese, B.F. Chmelka, G.D. Stucky, Nature 396 (1998) 152.
[31] P. Yang, D. Zhao, D. Margolese, B.F. Chmelka, G.D. Stucky, Chem. Mater. 11 (1999) 2831.
[32] M. Hartmann, A. Vinu, Langmuir 18 (2002) 8010.
[33] Y. Yue, A. Gédéon, J.-L. Bonardet, N. Melosh, J.-B. D' Espinose, J. Fraissard, Chem. Commun. (1999) 1967.
[34] A. Vinu, W. Böhlmann, V. Murugesan, M. Hartmann, J. Phys. Chem. B 108 (2004) 11496.
[35] A. Vinu, B.M. Devassy, S.B. Halligudi, W. Böhlmann, M. Hartmann, Appl. Catal. A-Gen. (2005) in press.
[36] J.H. Clark, A.P. Kybett, D.J. Macquarrie, S.J. Barlow, P. Landon, J. Chem. Soc., Chem. Commun. (1989) 1353.
[37] C.N. Rhodes, D.R. Brown, J. Chem. Soc., Faraday Trans. 89 (1993) 1387.
[38] P. Meric, A. Finiels, P. Moreau, J. Mol. Catal. A-Gen. 189 (2002) 251.